

Title	The Deficiency of indoleamine 2,3-Dioxygenase aggravates the CCl4 -Induced liver fibrosis in mice
Author(s)	Ogiso, Hideyuki; Ito, Hiroyasu; Ando, Tatsuya; Arioka, Yuko; Kanbe, Ayumu; Ando, Kazuki; Ishikawa, Tetsuya; Saito, Kuniaki; Hara, Akira; Moriwaki, Hisataka; Shimizu, Masahito; Seishima, Mitsuru
Citation	PLOS ONE (2016), 11(9)
Issue Date	2016-09-06
URL	http://hdl.handle.net/2433/217097
Right	© 2016 Ogiso et al. This is an open access article distributed under the terms of the Creative Commons Attribution License, which permits unrestricted use, distribution, and reproduction in any medium, provided the original author and source are credited.
Type	Journal Article
Textversion	publisher

RESEARCH ARTICLE

The Deficiency of Indoleamine 2,3-Dioxygenase Aggravates the CCl₄-Induced Liver Fibrosis in Mice

Hideyuki Ogiso¹, Hiroyasu Ito^{1*}, Tatsuya Ando¹, Yuko Arioka¹, Ayumu Kanbe¹, Kazuki Ando¹, Tetsuya Ishikawa³, Kuniaki Saito⁴, Akira Hara⁵, Hisataka Moriwaki², Masahito Shimizu², Mitsuru Seishima¹

1 Department of Informative Clinical Medicine, Gifu University Graduate School of Medicine, Gifu, Japan, **2** First Department of Internal Medicine, Gifu University Graduate School of Medicine, Gifu, Japan, **3** Department of Medical Technology, Nagoya University School of Health Sciences, Nagoya, Japan, **4** Human Health Sciences, Kyoto University Graduate School of Medicine and Faculty of Medicine, Kyoto, Japan, **5** Department of Tumor Pathology, Gifu University Graduate School of Medicine, Gifu, Japan

* hito@gifu-u.ac.jp



OPEN ACCESS

Citation: Ogiso H, Ito H, Ando T, Arioka Y, Kanbe A, Ando K, et al. (2016) The Deficiency of Indoleamine 2,3-Dioxygenase Aggravates the CCl₄-Induced Liver Fibrosis in Mice. *PLoS ONE* 11(9): e0162183. doi:10.1371/journal.pone.0162183

Editor: Bernhard Ryffel, Centre National de la Recherche Scientifique, FRANCE

Received: April 16, 2016

Accepted: August 18, 2016

Published: September 6, 2016

Copyright: © 2016 Ogiso et al. This is an open access article distributed under the terms of the [Creative Commons Attribution License](https://creativecommons.org/licenses/by/4.0/), which permits unrestricted use, distribution, and reproduction in any medium, provided the original author and source are credited.

Data Availability Statement: All relevant data are within the paper and its Supporting Information files.

Funding: The authors did not receive specific funding for this work.

Competing Interests: The authors have declared that no competing interests exist.

Abbreviations: ECM, extracellular matrix; HSC, hepatic stellate cell; IDO, indoleamine 2,3-dioxygenase; DCs, dendritic cells; TNF, tumor necrosis factor; IL, interleukin; Tregs, regulatory T cells; CCl₄, carbon tetrachloride; 1-MT, 1-methyl-DL-tryptophan; WT, wild-type; IDO-KO, IDO-knockout; α-

Abstract

In the present study, we examined the role of indoleamine 2,3-dioxygenase (IDO) in the development of CCl₄-induced hepatic fibrosis. The liver fibrosis induced by repetitive administration with CCl₄ was aggravated in IDO-KO mice compared to WT mice. In IDO-KO mice treated with CCl₄, the number of several inflammatory cells and the expression of pro-inflammatory cytokines increased in the liver. In the results, activated hepatic stellate cells (HSCs) and fibrogenic factors on HSCs increased after repetitive CCl₄ administration in IDO-KO mice compared to WT mice. Moreover, the treatment with L-tryptophan aggravated the CCl₄-induced hepatic fibrosis in WT mice. Our findings demonstrated that the IDO deficiency enhanced the inflammation in the liver and aggravated liver fibrosis in repetitive CCl₄-treated mice.

Introduction

Hepatic fibrosis is a wound-healing response to various chronic hepatic injuries resulting from viral infection (particularly hepatitis B and C), alcohol abuse, drugs, metabolic diseases, or autoimmune diseases [1]. Continued progression of hepatic fibrosis results in liver cirrhosis and may cause chronic hepatic failure or liver cancer [2]. Hepatic fibrosis is characterized by the deposition of extracellular matrix (ECM), including type I and III collagens, glycoproteins and proteoglycans [3]. ECM deposition is increased due to excessive ECM production and reduced ECM degradation in the liver. The most important event in hepatic fibrosis is the activation of hepatic stellate cells (HSCs). Following liver injury of any etiology, HSCs undergo a response activation, which involves the transition of quiescent cells into proliferative and fibrogenic myofibroblasts. Such activated HSCs are then able to produce ECM in the liver [1].

SMA, alpha-smooth muscle actin; ALT, plasma alanine aminotransferase; PBS, phosphate-buffered saline; BSA, bovine serum albumin; ACTA2, alpha smooth muscle actin2; Col1a2, collagen Type I Alpha2; MNC, intrahepatic mononuclear cell; NK, natural killer; NASH, non-alcoholic steatohepatitis.

Indoleamine 2,3-dioxygenase (IDO) has been identified as a powerful immunomodulatory molecule with significant enzymatic activity for catabolism of the essential amino acid L-tryptophan [4,5]. IDO is expressed in epithelial cells, macrophages, and dendritic cells (DCs), and is up-regulated by pro-inflammatory cytokines, including interferon- γ , tumor necrosis factor (TNF)- α and interleukin (IL)-6 [6]. Previous reports indicated that IDO expression of the liver was enhanced in acute hepatitis model [7,8]. IDO activity has been found to greatly impact immune tolerance and immune regulation [9]. The immunosuppressive activity of IDO is derived from inhibition of T cell activation and proliferation in microenvironment, where tryptophan is decreased and tryptophan metabolites are increased [10]. Also, IDO can enhance regulatory T cells (Tregs) activity [11] and suppress host immune response via Tregs [12].

Pro-inflammatory cytokines, such as TNF- α and IL-6, have been shown to increase in the liver of carbon tetrachloride (CCl₄)-induced hepatitis [13]. Pro-inflammatory cytokines and chemokines stimulate HSCs, which produce ECM in the liver. Thus, liver fibrosis is closely related to liver inflammation. Therefore, IDO induced by various pro-inflammatory cytokines may be involved in the attenuation of liver fibrosis. We indicated in a previous report that IDO attenuated liver injury in an α -galactosylceramide-induced hepatitis model [4]. Moreover, a recent report demonstrated that the inhibition of IDO activity by 1-methyl-DL-tryptophan (1-MT) exacerbated CCl₄-induced liver injury [14]. However, the role of IDO in the development of liver fibrosis remains unclear. In the present study, we examined the effect of IDO on CCl₄-induced liver fibrosis in mice and demonstrated that the deficiency of IDO aggravates the development of liver fibrosis.

Materials and Methods

Mice

Male C57BL/6J wild-type (WT) mice (age, 6–8 weeks) were obtained from Japan SLC (Shizuoka, Japan). IDO-knockout (IDO-KO) mice with a C57BL/6J background were obtained from The Jackson Laboratory (Bar Harbor, ME). Mice were maintained at the specific pathogen free unit under 12 h light-dark cycle at 23°C. Mice were provided free access to food and water. The food was obtained from Japan SLC (Shizuoka, Japan). The study protocols were approved by the Ethics Committee for Animal Experiments of Gifu University. All protocols were in accordance with guidelines established by the National Institutes of Health Guide for Care and Use of Laboratory Animals.

Animal Experiments

Mice received intraperitoneal injections of a 10% CCl₄ (Wako, Osaka, Japan) solution in olive oil (1 μ g/g body weight) twice a week for 6 weeks, while control mice were administered only olive oil. In some experiments, mice were intraperitoneally administered with L-tryptophan (Wako, Osaka, Japan) or L-kynurenine (Sigma-Aldrich, St Louis, MO) twice a week for 6 weeks. Mice were sacrificed by cervical dislocation 7 days after the final administration of CCl₄, and necropsy was performed. In another group, mice were administered a single dosage of 10% CCl₄ solution in olive oil (1 μ g/g body weight) intraperitoneally and were sacrificed in a similar manner at day 0, day 1, day 3 and day 6 post-administration.

Histology and Immunohistochemistry

Tissue samples were fixed in 10% buffered formalin and embedded in paraffin. The 4 μ m thick sections of the livers were stained with hematoxylin-eosin. To assess collagen deposition (fibrosis), 4 μ m thick sections of the livers were processed by Azan staining using a standard

histological procedure [15]. Also, 4 μm thick sections of the livers were stained by Picrosirius Red Stain Kit (Polysciences, Philadelphia, PA). The degree of fibrosis was evaluated semi-quantitatively using the ImageJ program (National Institute of Health). Immuno-histochemical staining for α -smooth muscle actin (α -SMA) was used to evaluate activation of HSCs in the liver, as previously described [16,17]. Briefly, sections were deparaffinized and treated with 3% hydrogen peroxide to inactivate endogenous peroxidases. Sections were heated in 0.1 M citrate buffer (pH 6.0), using the Pascal Heat Induced Antigen Retrieval System (Dako, Grostrup, Denmark). Non-specific antibody binding sites were blocked in phosphate-buffered saline (PBS, pH 7.4) containing 2% bovine serum albumin (BSA, Wako Pure Chemical Industries, Osaka, Japan) for 30 min. The sections were then incubated with rabbit anti α -actin monoclonal antibody (ab5694, Abcam, Tokyo, Japan) diluted 1/850 in PBS and incubated overnight at 4°C. Sections were incubated with rabbit immunoglobulin antibody (E0432, Dako, Grostrup, Denmark) diluted 1/300 in PBS. α -SMA protein was observed by using a labelled streptavidin-biotin kit (Dako, Grostrup, Denmark) containing biotinylated antibody and peroxidase-labeled streptavidin. The peroxidase binding sites were detected by staining with 3,3'-diaminobenzidine. Finally, samples were counterstained using Mayer's hematoxylin.

Sircol™ Collagen Assay

The collagen content in the liver tissues was determined using the Sircol™ Collagen Assay (Bio-color Ltd., UK), according to the manufacturer's protocol. This assay uses Sirius Red, an anionic dye with sulfonic acid side chain groups, which reacts with the basic amino acids present in collagen. Briefly, liver tissues were homogenized and collagen was solubilized in 0.5 M acetic acid. Tissue extracts were incubated with the Sirius Red dye and absorbance was determined with a microplate reader (BIORAD, Hercules, CA) at a wavelength of 540 nm. The amount of collagen was expressed as $\mu\text{g/g}$ wet tissue.

Analysis of liver transaminase

Hepatocyte damage was assessed at the indicated time points after CCl_4 injection through the measurement of plasma alanine aminotransferase (ALT) activities using an automated clinical analyzer (BM2250; JEOL, Tokyo, Japan).

Measurements of L-tryptophan

Liver tissue from the mice was mixed with 6 volume of 10% perchloric acid and homogenized. Next, homogenized liver tissue was subjected sonication by homogenizer (Sonifer: BRANSON, Danbury, CT). After centrifugation, the concentrations of L-tryptophan in the supernatants were measured using HPLC with Brava C18-ODS Column ($150 \times 4.6\text{mm}$ $3\mu\text{m}$; GRACE, Columbia, United States) and a spectrophotometric detector or a fluorescence spectrometric detector as described previously [18]. UV signals were monitored at 280 nm for L-tryptophan. The mobile phase consisted of 2.5% acetonitrile in 0.1 M sodium acetate (pH 3.9) and was filtered through a 0.45- μm -pore HA-type filter obtained from Millipore (Bedford, MA). The flow rate was maintained 0.75ml/min throughout the chromatographic run.

Hepatic mononuclear cell preparation and flow cytometric analysis

Hepatic mononuclear cells (MNCs) were isolated as previously described [19]. Briefly, the excised liver was cut into small pieces with scissors, pressed through a 200-gauge stainless mesh, and suspended in PBS. Hepatic MNCs were separated from parenchymal hepatocytes and hepatocyte nuclei by Ficoll-Conray (IBL, Gunma, Japan) and washed twice in ice-cold

medium. Cell viability and cell numbers were assessed by trypan blue exclusion. For flow cytometry, liver MNCs were stained using a standard protocol. The following Abs were used: FITC conjugated Anti-mouse F4/80 mAb (Clone: BM8) and PE-Cy7 conjugated Anti-mouse CD11b mAb (Clone: M1/70). Samples were acquired on BD FACSCanto2 flow cytometer (BD Biosciences, San Diego, CA).

MACS cell preparation

CD11b⁺, CD11b⁻, CD11c⁺ and CD11c⁻ cells were isolated by MACS Magnetic Bead columns (Miltenyi Biotec, Bergisch Gladbach, Germany) with antibodies against CD11b and CD11c, according to the manufacturer's instructions. Briefly, the cell pellet was suspended in 0.5ml of PBS, 0.5% bovine serum albumin, 2mM EDTA, followed by addition of anti CD11b or CD11c magnetic beads and incubated at 4°C for 15min. CD11b⁺, CD11b⁻, CD11c⁻/CD11c⁺, and CD11b⁻/CD11c⁻ cells were isolated by MACS Magnetic Bead Column.

HSCs isolation

HSCs were isolated from the mouse liver as described previously with a minor modification [20]. Briefly, the mouse liver was perfused with Liver Perfusion Medium at 37°C, followed by Liver Digest Medium (Invitrogen, NY). The digested liver was excised and minced with scissors. The resulting suspension was filtered through a stainless steel mesh (150 µm diameter). The suspension was centrifuged at 50 × g for 2 min at 4°C. The supernatant, including HSCs, was suspended in a 15% iodixanol (Optiprep, Oslo, Norway) solution. Few percent of 10% iodixanol solution and PBS were then layered on to the cell suspension, and HSCs were corrected at the interface between 10% iodixanol and PBS were corrected after centrifugation at 1,400 × g for 20 min at 4°C.

Quantitative real-time reverse transcription-polymerase chain reaction analysis

Total RNA was extracted from mouse liver tissues or isolated HSCs using Isogen II (Nippon-gene, Tokyo, Japan) and then transcribed to cDNA using the High Capacity cDNA Transcription Kit (Applied Biosystems, Foster City, CA) according to the manufacturer's protocol. From each sample, 1 µg of total RNA was used as a template for cDNA synthesis. The resulting cDNA was used as a template for real-time polymerase chain reaction (PCR) conducted using pre-designed primer/probe sets for IDO1, IL1-β, IL-6, TNF-α, CCL2, PDGF-β, Col1a2, ACTA2, Timp-1, and 18S rRNA (Applied Biosystems) and Twinbird Probe qPCR Mix (TOYOBO, Osaka, Japan) for Taqman Gene Expression Assays. 18S rRNA was used as an internal control. Real-time PCR was performed using the Light-Cycler Rapid Thermal Cycler System (Roche Diagnostic Systems, Indianapolis, IN). For evaluation of mRNA expression of CYP1a2, CYP2e1, we analyzed on Light Cycler Rapid Thermal Cycler System using the KAPA SYBR Fast qPCR kit (KAPA BIOSYSTEMS). Primers for RT-qPCR used in this study were as follows;

Cyp1a2-fw: TGGAGCTGGCTTTGACACAG, CYP1a2-rv: CGTTAGGCCATGTCACAAGTAGC,
Cyp2e1-fw: AAGCGCTTCGGGCCAG, Cyp2e1-rv: TAGCCATGCAGGACCACGA.

Statistical analysis

The data are expressed as the mean ± standard error of the mean (SEM). Statistical significance of the differences between two groups were determined using Student's t-test, and those among

three groups were tested using one-way analysis of variance (ANOVA). The criterion for statistical significance was $P < 0.05$.

Results

IDO1 expression and IDO activity were up-regulated after CCl₄ administration

In a previous study, IDO1 expression was enhanced in the liver of hepatitis model [7]. We measured the expression of IDO1 mRNA in the liver 24 hours after CCl₄ administration by quantitative real-time RT-PCR. IDO1 mRNA expression was significantly increased in WT mice after CCl₄ administration (Fig 1A). Meanwhile, IDO1 mRNA expression was not detected in IDO-KO mice. Previously report indicated myeloid CD11c⁺ dendritic cells express IDO at the inflammatory border [21]. To address which type of cell expresses IDO1 after CCl₄ administration, we isolated CD11b⁺ ($5.3 \pm 1.4 \times 10^5$ / liver), CD11b⁻ ($25.7 \pm 4.9 \times 10^5$ / liver), CD11b⁻/CD11c⁻ ($25.5 \pm 4.8 \times 10^5$ / liver), and CD11b⁻/CD11c⁺ ($0.2 \pm 0.1 \times 10^5$ / liver) cells from hepatic MNCs of CCl₄-administrated mice using MACS system. Subsequently, we examined the mRNA expression of IDO1 in each cell population using real-time RT-PCR. IDO1 expression was significantly higher in CD11b⁻ cells and CD11b⁻/CD11c⁺ cells after the treatment of CCl₄ (Fig 1B). Therefore, these results indicated that CD11b⁻/CD11c⁺ cells mainly expressed IDO1 mRNA after CCl₄ administration.

IDO is the enzyme which catabolizes L-tryptophan to L-kynurenine. To evaluate the IDO activity, we measured L-tryptophan levels in the liver. L-tryptophan levels in the liver tissue from WT mice were significantly reduced after CCl₄ administration (Fig 1C). In contrast, L-tryptophan levels in the liver of IDO-KO mice were not reduced after CCl₄ administration.

The CCl₄-induced liver injury and hepatic fibrosis in IDO-KO mice was exacerbated compared to that in WT mice

To evaluate the role of IDO in CCl₄-induced liver injury, we measured serum ALT activity in WT and IDO-KO mice after single administration of CCl₄ to WT and IDO-KO. Serum ALT levels in IDO-KO mice significantly increased 24 hours after CCl₄ injection compared with those in WT mice (Fig 1D). Histological examination also indicated that inflammatory response in IDO-KO was exacerbated compared with that in WT mice after the administration of CCl₄ (Fig 1E). Cell number of hepatic MNCs was significantly increased in IDO-KO mice compared to WT mice 24 hours after CCl₄ administration (Fig 1F).

CCl₄ is metabolized by cytochrome P450 in endoplasmic reticulum of the liver. To dismiss the possibility of the difference between WT mice and IDO-KO in the liver cytochrome level, we investigated the cytochrome level (CYP1A2 and CYP2E1) in the liver of WT and IDO-KO mice. There was no difference of these cytochrome expression levels in the liver between WT mice and IDO-KO mice (S1 Fig).

To evaluate the effect of IDO on CCl₄-induced hepatic fibrosis, WT mice and IDO-KO mice were treated with CCl₄ twice a week for 6 weeks. All mice were sacrificed at 7 days after the last administration of CCl₄. The liver sections were stained by Azan staining. Histological analysis showed that collagen deposition around Glisson's sheath in the IDO-KO mice increased after CCl₄ treatment compared to that in WT mice (Fig 2B). Evaluation of fibrosis was quantified based on the aniline blue-positive fibrotic area in five random fields on Azan staining sections of liver from each group. The aniline blue-positive areas in IDO-KO mouse tissue was significantly increased compared to that of the WT mice (Fig 2C). Because hepatic fibrosis is the result of the accumulation of ECM including collagen, we then measured the

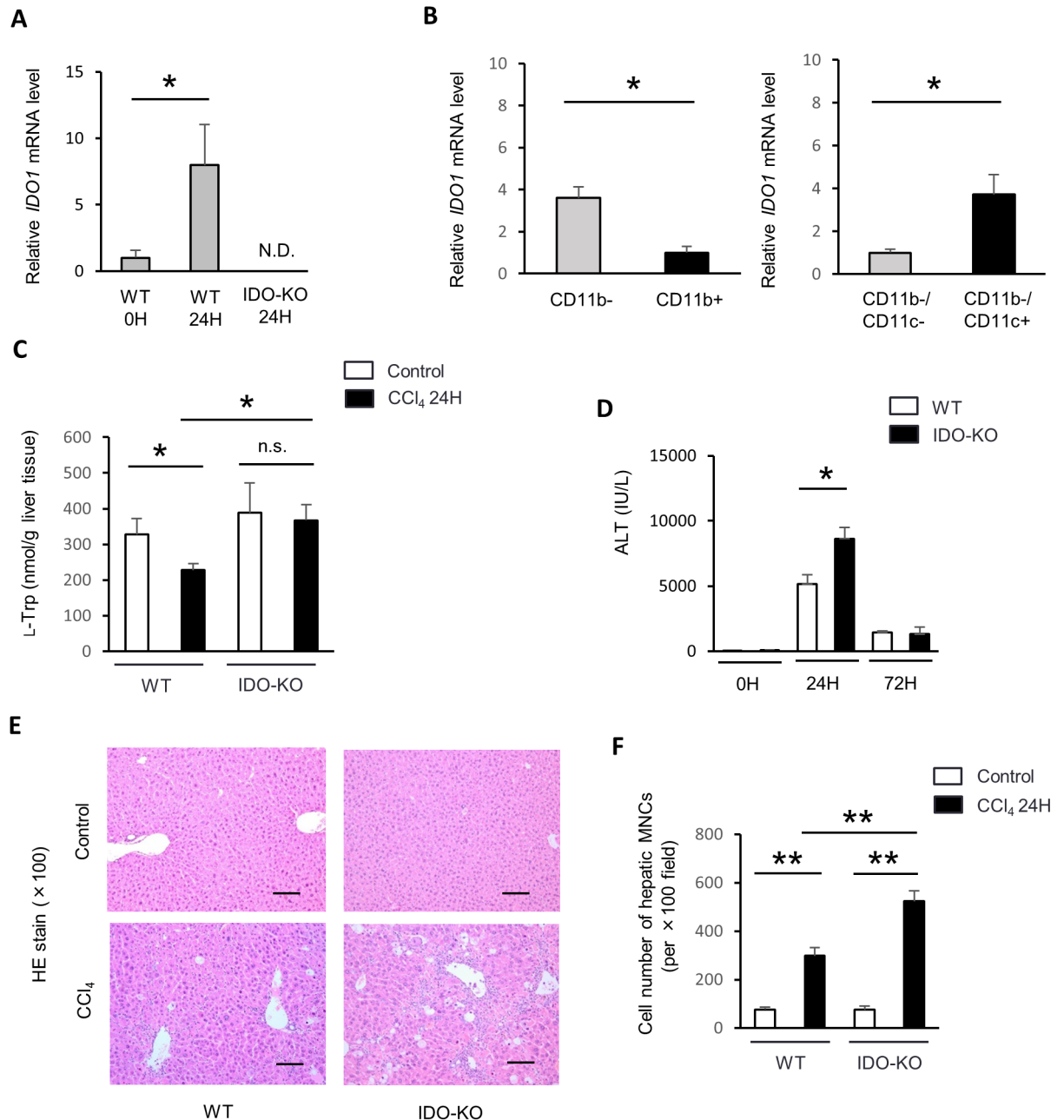


Fig 1. IDO expression and activity were up-regulated after CCl₄ administration in WT mice. Male C57BL/6J WT mice (n = 3) and IDO-KO mice (n = 3) were treated with CCl₄ (1 mL/kg, 10% diluted in olive oil). The control group mice (WT mice, n = 3 and IDO-KO mice, n = 3) were injected with olive oil alone. All mice were sacrificed at 24 hours after the administration of CCl₄ or olive oil alone. (A) mRNA expressions of IDO1 in the liver were measured by quantitative real-time RT-PCR. The results were normalized to the expression of 18S rRNA. (B) mRNA expression of IDO1 in CD11b⁻ cells, CD11b⁺ cells, CD11c⁻ cells and CD11c⁺ cells in the liver of CCl₄ induced injury. WT mice (n = 3) mice were treated with a single CCl₄ dosage (1 mL/kg, 10% diluted in olive oil). Hepatic MNCs were subjected MACS cell preparation with CD11b⁻ and CD11b⁺ cells 24 hours after CCl₄ administration. Also too, hepatic MNCs were subjected MACS cell preparation with CD11c⁻ and CD11c⁺ cells. (C) The concentrations of L-tryptophan in supernatants of liver homogenates were measured using HPLC (n = 3–5: each group). (D) Serum ALT levels in WT or IDO-KO mice were measured 0, 24, and 72 hours after CCl₄ administration (n = 3–7: each group). (E) Representative photomicrographs of liver sections at 24 hours after CCl₄ administration stained with hematoxylin-eosin, ×100 original magnification, Scale bars: 100 μm. (F) The cell number of hepatic MNCs at 24 hours after CCl₄ administration per ×400 field (n = 3: each group). Each column and error bar represents the mean and SEM, respectively, of results for triplicate samples. * indicate statistically significant differences, at P<0.05.

doi:10.1371/journal.pone.0162183.g001

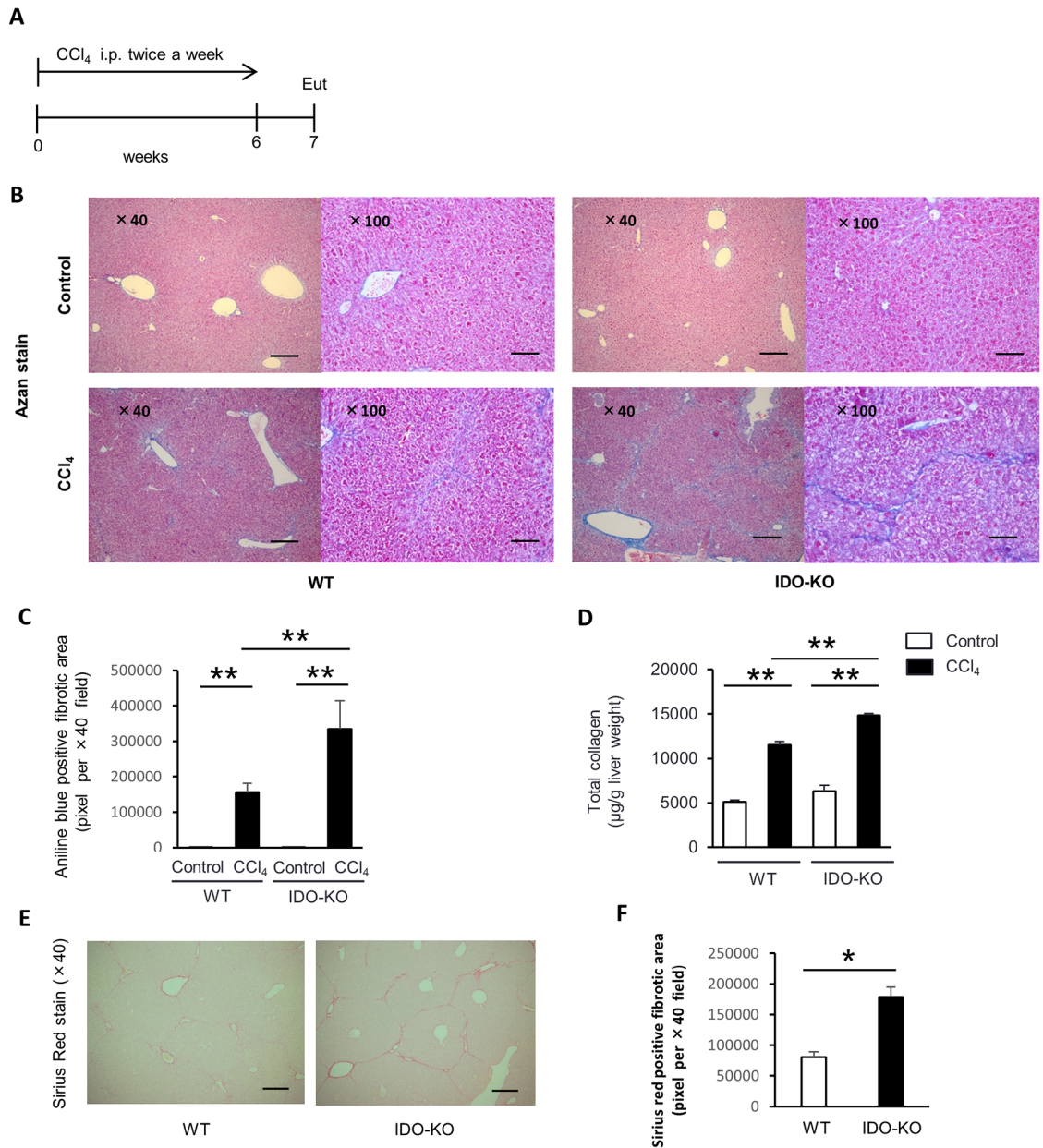


Fig 2. CCl₄-induced hepatic fibrosis was exacerbated in IDO-KO mice compared to WT mice. Male C57BL/6J WT mice (n = 4) and IDO-KO mice (n = 5) were treated with CCl₄ (1 mL/kg, 10% diluted in olive oil) twice a week for 6 weeks. All mice were sacrificed at 7 days after the last administration of CCl₄. The control group mice (WT mice, n = 5 and IDO-KO mice, n = 5) were injected with olive oil alone. (A) The diagram showing experimental design. Eut, euthanasia. (B) Representative photomicrographs of experimental mice liver sections of Azan staining, left panel: ×40 original magnification, Scale bars: 250 µm, right panel: ×100 original magnification, Scale bars: 100 µm. (C) Evaluation of fibrosis was quantified based on the aniline blue-positive fibrotic area in five random fields on the liver tissue sections for each group using ImageJ software. (D) The total collagen content in the liver tissue after the repeatedly CCl₄ administration was measured using a Sircol™ Collagen Assay. (E) Representative photomicrographs of repeatedly CCl₄-treated mice liver sections stained with Sirius red, ×40 original magnification, Scale bars: 250 µm. (F) Evaluation of fibrosis was quantified based on the Sirius red-positive fibrotic area in five random fields on the liver tissue sections for each group using ImageJ software. Each column and error bar represents the mean and SEM, respectively, of results for triplicate samples. * indicate statistically significant differences, at P<0.05. ** indicate statistically significant differences, at P<0.01.

doi:10.1371/journal.pone.0162183.g002

level of total collagen in the liver tissue of WT mice and IDO-KO mice treated with CCl₄. The total collagen level in the livers from the IDO-KO mice was significantly increased compared to those from WT mice after CCl₄ treatment (Fig 2D). Aniline blue stains not only collagen-deposition area but also basement membrane mucin in Azan staining method. Sirius red staining shows only collagenous structures as brilliant red-positive area. Therefore, we also stained the liver sections by Sirius red. The Sirius red-positive areas in IDO-KO mouse tissue was significantly increased compared to that of the WT mice (Fig 2E and 2F). Moreover, 1-MT treatment also promoted the liver fibrosis induced by repetitive administration with CCl₄ (S2 Fig).

mRNA expression of pro-inflammatory cytokines and fibrogenic factors after single administration of CCl₄

As previously reported, HSCs are activated by paracrine stimulation with various cytokines and chemokines released from hepatic parenchymal cells [22], Kupffer cells [23], neutrophils, and platelets [24]. Therefore, we conducted a detailed analysis of the mRNA expression of intrahepatic pro-inflammatory cytokines (IL-1 β , TNF- α , IL-6) 0, 1, 3, and 6 days after CCl₄ single injection using real time RT-PCR. Among pro-inflammatory cytokines, the mRNA expression of TNF- α in hepatic tissue was significantly higher in IDO-KO mice than in WT mice 1 day after administration of a single CCl₄ dosage (Fig 3). The mRNA expression of IL-1 β was also increased in IDO-KO mice compared to WT mice 6 days after CCl₄ injection. Monocyte and macrophage migrate toward inflamed tissues under the influence of CCL2 and produce TNF- α in inflamed tissues [25]. Therefore, we analyzed the mRNA expression of CCL2. The mRNA expression of CCL2 in hepatic tissue was significantly higher in IDO-KO mice than in WT mice. Moreover, we measured mRNA expression of fibrotic factor (PDGF- β) in hepatic tissue. mRNA expression of PDGF- β was significant higher in IDO-KO mice than WT mice 6 days after administration of single CCl₄ dosage (Fig 3).

F4/80+CD11b+ cells was significantly increased in IDO-KO mice compared to WT mice after CCl₄ administration

As previously reported, F4/80+CD11b+ cells produced TNF- α [26]. The mRNA expression of TNF- α in hepatic tissue was significantly higher in IDO-KO mice than WT mice 24 h after single CCl₄ administration (Fig 3). Moreover, we investigated the frequency and cell number of F4/80+CD11b+ cells in the liver under the CCl₄-induced hepatic injury of WT or IDO-KO mice by flow cytometer. The frequency and cell number of F4/80+CD11b+ cells were significantly increased in IDO-KO mice compared to WT mice 24 hours after CCl₄ administration (Fig 4A–4C). Next, we also examined the phenotypes of the other immune cells after CCl₄ administration (S3 Fig). There was no difference between CCl₄-treated WT mice and CCl₄-treated IDO-KO mice in the frequency of CD4+, CD8+, natural killer (NK), and NKT cells in the liver. The number of these cells in IDO-KO increased compared to that in WT mice after the administration with CCl₄.

An increased number of α -SMA-positive HSCs in IDO-KO mice observed compared to that in WT mice

During the process of liver fibrosis, activated HSCs undergo increased collagen production. Because activated HSCs express α -SMA, we performed immunohistochemical staining of α -SMA in liver sections from the WT and IDO-KO mice treated with CCl₄ repeated injection for 6 weeks. The number of α -SMA positive cells per field of the liver section was significantly greater in the IDO-KO mice compared to that in WT mice (Fig 5B and 5C).

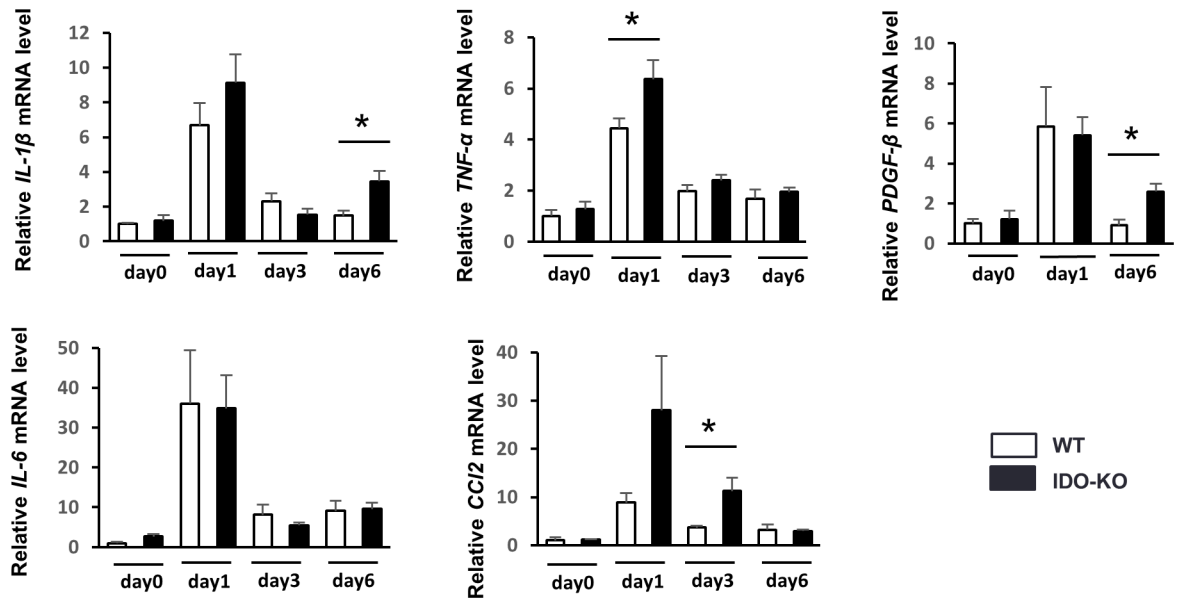


Fig 3. mRNA expression of pro-inflammatory cytokines and fibrogenic factors after single administration of CCl₄. WT mice and IDO-KO mice were treated with a single CCl₄ dosage (1 mL/kg, 10% diluted in olive oil) (n = 5: each group). The control group (WT mice and IDO-KO mice) was injected with olive oil alone (n = 3: each group). The relative expression levels of IL-1β, TNF-α, IL-6, CCL2, and PDGF-β mRNA in the liver were measured on day 0, 1, 3 and 6 after CCl₄ administration using quantitative real time RT-PCR. The results were normalized to the expression of 18S rRNA. Each column and error bar represents the mean and SEM, respectively, of results for triplicate samples. * indicate statistically significant differences, at P<0.05.

doi:10.1371/journal.pone.0162183.g003

ACTA2, Col1a2, and Timp-1 mRNA expression in HSCs of IDO-KO mice is increased following CCl₄ treatment compared with that of WT mice

As previously described, HSCs are activated by various pro-inflammatory cytokines [27]. Subsequently, activated HSCs express ACTA2, Col1a2, and Timp-1, and product extracellular matrix. Therefore, we assessed the ACTA2, Col1a2, and Timp-1 expression in HSCs. WT mice and IDO-KO mice were treated with CCl₄ twice a week for 8 weeks. All mice were sacrificed 3 days after the last administration of CCl₄. HSCs were isolated from the liver using density-gradient centrifugation. Next, we determined the mRNA expression of ACTA2, Col1a2, and Timp-1 in HSCs using quantitative real time RT-PCR. ACTA2 and Col1a2 mRNA expression was greater in IDO-KO mice compared to that in WT mice after treatment with CCl₄ (Fig 5E).

The administration of L-tryptophan aggravated CCl₄-induced liver fibrosis in WT mice

Next, we examined the role of L-tryptophan and L-kynurenine in the development of CCl₄-induced liver fibrosis. The administration of CCl₄ induced the activation of IDO and decreased L-tryptophan in WT mice. On the other hand, we predict that L-tryptophan metabolites such as L-kynurenine in CCl₄-treated IDO-KO mice are decreased compared to that in CCl₄-treated WT mice. Therefore, to investigate the role of L-tryptophan and L-kynurenine in the development of liver fibrosis, we repeatedly administered L-tryptophan into CCl₄-treated WT mice and L-kynurenine in CCl₄-treated IDO-KO mice. And we stained the liver sections by Sirius red. The administration of L-kynurenine did not affect the Sirius red-positive areas in CCl₄-

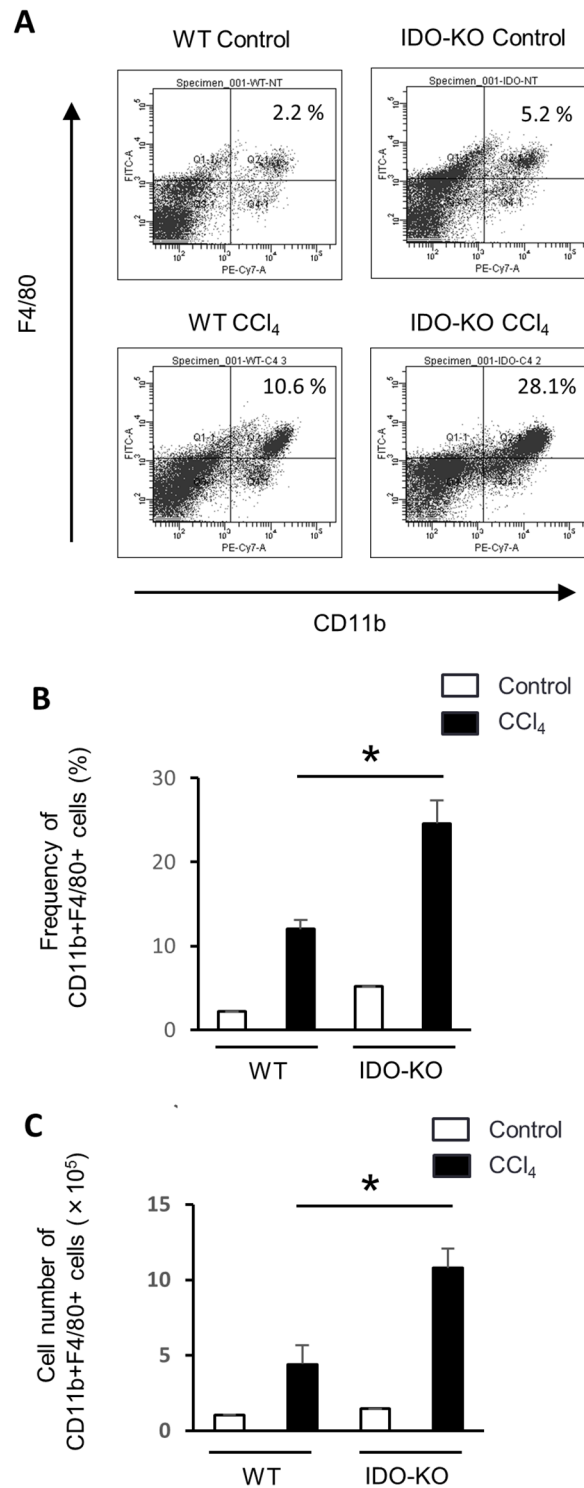


Fig 4. The frequency and cell number of F4/80+CD11b+ cells after single administration of CCl₄. (A) FACS analysis of F4/80+CD11b+ cells in hepatic MNCs after the administration with CCl₄. WT mice (n = 3) and IDO-KO mice (n = 3) were treated with CCl₄ injection (1 mL/kg, 10% diluted in olive oil). Control group (WT mice and IDO-KO mice) were administrated with olive oil alone. All mice were sacrificed at 24 hours after the administration of CCl₄ or olive oil alone. Representative flow cytometry data were presented. (B) The frequency of F4/80+CD11b+ cells in the liver of WT and IDO-KO mice treated with CCl₄ administration. (C) The cell number of F4/80+CD11b+ cells in the liver of WT and IDO-KO mice treated with CCl₄ administration.

The total cell number of F4/80+CD11b+ cells in the liver of WT and IDO-KO mice treated with CCl₄ administration. Each column and error bar represents the mean and SEM, respectively, of triplicate samples. * indicates statistically significant difference at P<0.05.

doi:10.1371/journal.pone.0162183.g004

treated IDO-KO mice. On the other hand, the administration of L-tryptophan significantly increased the Sirius red-positive areas in CCl₄-treated WT mice (Fig 6).

Discussion

In the present study, we found that hepatic fibrosis in IDO-KO mice was exacerbated by repeated administration of CCl₄ compared to that in WT mice. CCl₄ treatment induces various pro-inflammatory cytokines in the liver. TNF- α mRNA expression in IDO-KO mice significantly increased after single administration with CCl₄ compared with that in WT mice. The cell number of macrophages (F4/80+CD11b+ cells), which produce TNF- α , were significantly increased in IDO-KO mice compared to WT mice after CCl₄ administration. Moreover, HSCs in IDO-KO mice were more activated and produced more ACTA2 and Col1a2 after repeated administration with CCl₄. Thus, the deficiency of IDO expression enhanced the development of the liver fibrosis via the activation of HSCs.

The mechanism for CCl₄-induced liver injury and fibrosis has been studied extensively. Kupffer cells recognize dying hepatocytes induced by CCl₄ injection, and subsequently, produce chemical mediators, such as prostaglandins, leukotrienes, platelet-activating factors, and pro-inflammatory cytokines, including TNF- α and IL-1 β [28]. These signaling molecules induce the influx of leukocytes, including macrophages, neutrophils, and T cells into the necrotic area. These inflammatory cells produce cytokines that cause the proliferation of remaining viable hepatocytes as well as the transformation of HSCs into myofibroblasts to stimulate the repair process. Activated HSCs produce ECM, resulting in the liver fibrosis. Thus, the inflammatory response is a key component in liver fibrosis induced by the repeated administration of CCl₄. In general, IDO is also related to inflammatory response because IDO expression is markedly increased by pro-inflammatory cytokines. A previous study demonstrated that the administration of CCl₄ markedly induced IDO enzyme activity in the liver [14]. Similarly, IDO1 mRNA expression in the liver was increased in WT mice after CCl₄ administration in the present study (Fig 1A). Moreover, CD11b-/CD11c+ cells (dendritic cells) mainly expressed IDO1 mRNA after CCl₄ administration (Fig 1B). L-tryptophan levels in the liver tissue from WT mice were significantly reduced after CCl₄ administration (Fig 1C). Therefore, CCl₄ administration increased IDO expression and enhanced IDO activity in WT mice.

Recent study demonstrated that the inhibition of IDO activity by oral 1-MT administration could aggravate CCl₄-induced liver injuries [14]. In the present study, the liver injury in IDO-KO mice treated with CCl₄ was exacerbated compared with that in WT mice (Fig 1D–1F). CCl₄ is metabolized primarily by the cytochrome P450 of the hepatic oxidase system to trichloromethyl radicals [29]. The trichloromethyl radicals initiate the peroxidation of polyunsaturated fatty acids in the endoplasmic reticulum and mitochondria, and destroy the biomembrane structure [30]. Cytochrome P450 have high specificity of substrate and especially cytochrome P450 2E1 (CYP2E1) metabolize CCl₄ [31]. CYP2E1 level in the liver among WT mice and IDO-KO mice was not significantly difference (S1 Fig). Therefore, the difference of liver injury level between WT mice and IDO-KO mice after the administration with CCl₄ might be not due to the difference of cytochrome level.

Our findings also indicated that IDO deficiency enhanced the expression of pro-inflammatory cytokines after the administration of CCl₄ (Fig 3). Previous reports demonstrated that

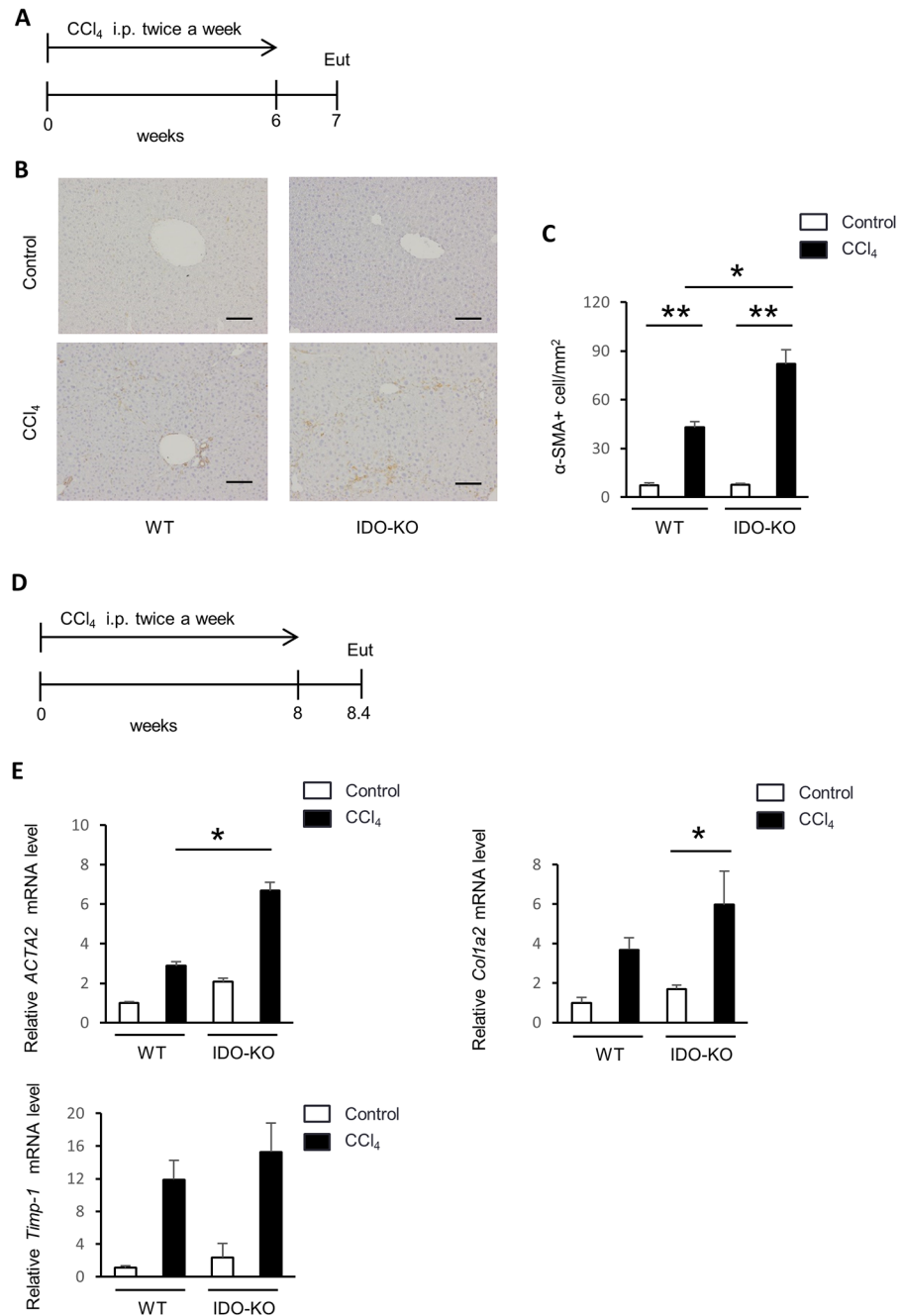


Fig 5. The number of α -SMA-positive HSCs was greater in IDO-KO mice compared to WT mice. WT mice (n = 4) and IDO-KO mice (n = 5) were treated with CCl₄ (1 mL/kg, 10% diluted in olive oil) twice a week for 6 weeks. All mice were sacrificed 7 days after the last administration of CCl₄. The control group (WT mice: n = 5, IDO-KO mice: n = 5) was injected with olive oil alone. (A) The diagram showing experimental design of Figs 5B and 5C. (B) Immunohistochemical staining of α -SMA in the liver tissue sections from the experimental mice, $\times 100$ original magnification, Scale bar: 100 μ m. (C) The number of α -SMA-positive cells per field was counted in three fields from each liver tissue. (D) The diagram showing experimental design of Fig 5E. (E) ACTA2, Col1a2, and Timp-1 mRNA expression in HSC. WT mice and IDO-KO mice administered with vehicle or CCl₄ twice a week for 8 weeks. All mice were sacrificed at 3 days after the administration of CCl₄ or olive oil alone. HSCs were isolated from the mice liver. The relative expression level of ACTA2, Col1a2, and Timp-1 mRNA in HSCs was measured using quantitative real time RT-PCR. The results were normalized to the expression of 18S rRNA. Each column point and error bar represents the mean and SEM, respectively, of data from triplicate samples. * indicates statistically significant differences at *P<0.05.

doi:10.1371/journal.pone.0162183.g005

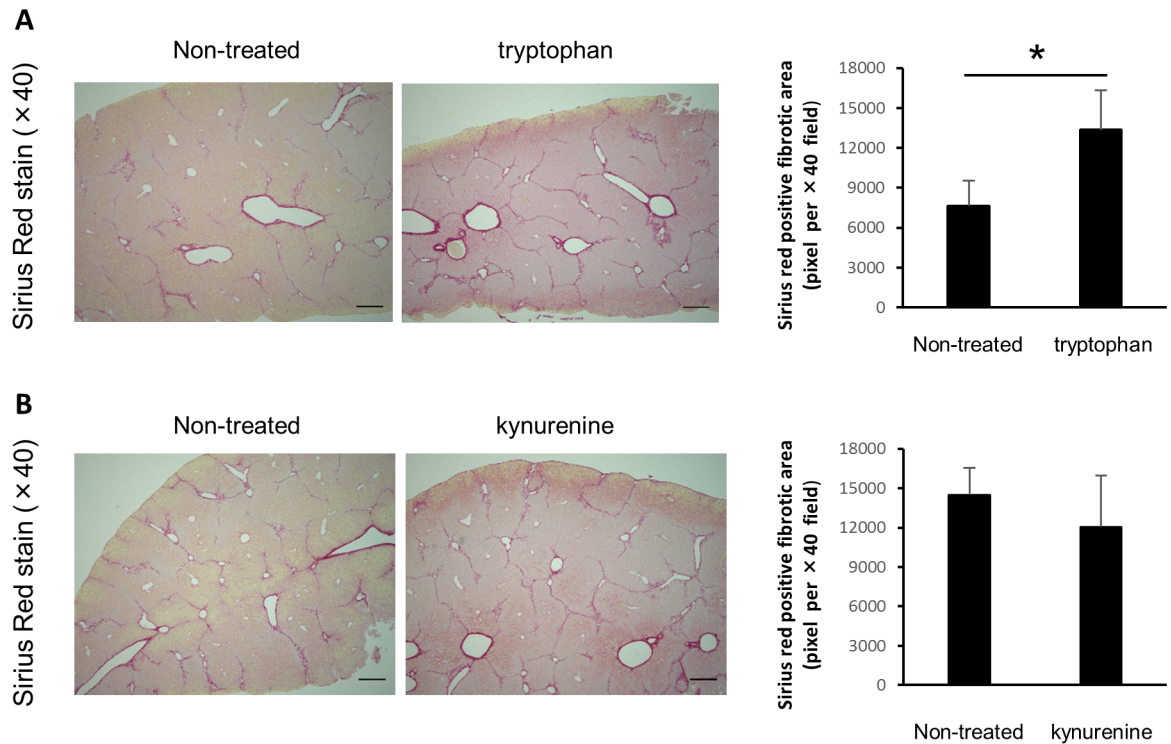


Fig 6. The effect of the administration with L-tryptophan and kynurenine on the development of liver fibrosis. WT mice (n = 8) were treated with CCl₄ (1 mL/kg, 10% diluted in olive. oil) or CCl₄ and L-tryptophan (1 mg / mouse) twice a week for 6 weeks. (B) IDO-KO mice (n = 8) were treated with CCl₄ (1 mL/kg, 10% diluted in olive oil) or CCl₄ and L-kynurenine (1 mg / mouse) twice a week for 6 weeks. Evaluation of fibrosis was quantified based on the Sirius red-positive fibrotic area in five random fields on the liver tissue sections for each group using ImageJ software. Each column and error bar represents the mean and SEM, respectively, of results for triplicate samples. * indicate statistically significant differences, at P<0.05.

doi:10.1371/journal.pone.0162183.g006

IDO suppressed inflammation in some experimental models [4,32,33]. Moreover, mRNA expression of PDGF-β in hepatic tissue was also significant higher in IDO-KO mice than WT mice 6 days after administration of CCl₄. Previous report demonstrated that IDO is induced after inflammatory stimulation and suppress the immune response in the host [9]. In the inflammatory state induced by CCl₄ injection, the expression of inflammatory cytokines increased and promptly restores to normal levels. The enhancement of cytokines expression during inflammatory states was often prolonged in IDO-KO mice [4]. In the present study, severe liver damage induced by CCl₄ injection enhanced the inflammation-related gene expression in early time point. In IDO-KO mice, the gene expression may increase in late time point (6 days after CCl₄ injection) because the IDO deficiency cannot induce enough immune suppression in mice. Thus, IDO deficiency enhanced the expression of pro-inflammatory cytokines and fibrogenic factors.

The increase of IDO expression has been shown to induce the decrease of tryptophan and the increase of tryptophan metabolites including kynurenine in the local microenvironment [34]. The activation of lymphocytes, specifically T cells and NK cells, requires sufficient tryptophan [10]. According to previous report, CCl₄-induced lymphocyte infiltration to the liver was ameliorated by pre-treating with berberine and improve liver damage [35]. In present study, the number of hepatic MNCs of IDO-KO mice (Ave. 4.4×10⁶) was significantly increased compared that of WT mice (Ave. 3.1×10⁶) after 24 hours after CCl₄ administration (data not shown). The number of hepatic MNCs of non-treat mice (WT and IDO-KO) was average

2.0×10^6 . Thus, we speculate that the deficiency of IDO increase the number of migrating lymphocyte to the liver, and aggravate liver damage. Therefore, the decrease of tryptophan in the local microenvironment suppresses the inflammatory response via the inhibition of lymphocyte activation. On the other hand, kynurenine has the ability to suppress lymphocyte activation and proliferation. The increase of kynurenine leads to the suppression of the inflammation induced by activated lymphocytes [36]. Thus, the induction of IDO suppresses the inflammatory response, and the inhibition of IDO activity aggregates the inflammation induced by activated lymphocytes. In the present study, as shown in Fig 6, the addition of L-tryptophan aggravated the liver fibrosis in CCl₄-treated WT mice. On the other hand, the administration with L-kynurenine did not affect the development of liver fibrosis in IDO-KO mice. These results indicated that IDO deficiency induced the increase of tryptophan level in the liver, and the increase of tryptophan level might induce liver inflammation via the activation of lymphocytes and aggravate the liver fibrosis.

It is well known that inflammation is fundamentally involved in the progression of liver fibrosis in chronic liver diseases. Liver fibrosis is induced in chronic viral hepatitis, alcohol-induced hepatitis, non-alcoholic steatohepatitis (NASH) and autoimmune hepatitis. Previous studies demonstrated that the suppression of liver inflammation reduced the progression of liver fibrosis [37]. Whereas various pro-inflammatory cytokines are increased during liver injury, TNF- α has particularly been shown to be involved in these liver diseases [19]. Pro-inflammatory cytokines can induce fibrogenic factors including TGF- β [38] and Col1a2 [39]. In the present study, expression TNF- α was increased in IDO-KO mice after injection of CCl₄ (Fig 3). In addition, the frequency and cell number of F4/80+CD11b+ cells were significantly increased in IDO-KO mice after CCl₄ administration (Fig 4A–4C). Also, IDO1 mRNA expression was induced in CD11b- cells and CD11c+ cells by CCl₄ administration (Fig 1B). Therefore, it indicated that CD11b- cells and CD11c+ cells expressed IDO1 by CCl₄ administration. IDO may suppressed the inflammatory response which induced by TNF- α .

Also, the number of activated HSCs was increased and the expression of ACTA2 and Col1a2 mRNA in HSCs were up-regulated in IDO-KO mice (Fig 5B, 5C and 5E). Thus, the IDO deficiency resulted in increased liver fibrosis induced by repeated administration of CCl₄ (Fig 2B–2D). The HSCs activation was induced by the repeated administration of CCl₄ (Fig 5B and 5C). ACTA2 and Col1a2 expression in HSCs was enhanced following CCl₄ injection in the IDO-KO mice (Fig 5E). Such repetitive stimulation with pro-inflammatory cytokine expression may lead to the induction of activated HSCs and the progression of liver fibrosis.

A recent study demonstrated that the induction of liver fibrosis and hepatocellular carcinoma is inhibited by the attenuation of liver inflammation during chronic viral hepatitis [40]. Previous study indicated that the IDO deficiency enhanced the liver injury in autoimmune hepatitis model (4). Our findings also demonstrated that the IDO deficiency enhanced the inflammation in the liver and aggravated liver fibrosis in CCl₄-induced liver injury model. Taken together, enhanced IDO expression in inflammatory state may delay the progression of liver fibrosis and possibly the development of hepatocellular carcinoma.

Supporting Information

S1 Fig. mRNA expression of cytochrome in the liver tissue of WT and IDO-KO mice. The relative expression levels of CYP1a2 and CYP2e1 mRNA in the liver were measured using quantitative RT-PCR. (TIF)

S2 Fig. The effect of IDO1 inhibitor, 1-MT, in CCl₄-induced hepatic fibrosis. Control group and 1-MT group (4 mg/ml dissolved alkaline water) were treated with CCl₄. (A)

Representative photomicrographs of experimental mice liver sections of Sirius red staining. Scale bars: 250 μ m. (B) Evaluation of fibrosis was quantified based on the sirius red-positive fibrotic area in five random fields on the liver tissue sections for each group using ImageJ software.

(TIF)

S3 Fig. The frequency and cell number of CD4+, CD8+, NK, and NKT cells after single administration of CCl₄. (A) The frequency of CD4+, CD8+, NK (DX5+), and NKT (CD3+/DX5+) cells in the liver of WT and IDO-KO mice treated with CCl₄ administration. (C) The cell number of CD4+, CD8+, NK, and NKT cells in the liver of WT and IDO-KO mice treated with CCl₄ administration.

(TIF)

Acknowledgments

We are grateful to Dr. M. Takamatsu, Division of Pathology, The Cancer Institute, Japanese Foundation for Cancer Research, Tokyo, Japan, for technical assistance.

Author Contributions

Conceptualization: HO HI.

Formal analysis: HO HI M. Shimizu KA TI HM.

Investigation: HO HI TA YA AK.

Methodology: KS AH.

Writing – original draft: HO HI M. Seishima.

References

1. Friedman SL (2000) Molecular regulation of hepatic fibrosis, an integrated cellular response to tissue injury. *J Biol Chem* 275: 2247–2250. PMID: [10644669](#)
2. Zhang DY, Friedman SL (2012) Fibrosis-dependent mechanisms of hepatocarcinogenesis. *Hepatology* 56: 769–775. doi: [10.1002/hep.25670](#) PMID: [22378017](#)
3. Fan X, Zhang Q, Li S, Lv Y, Su H, Jiang H, et al. (2013) Attenuation of CCl₄-induced hepatic fibrosis in mice by vaccinating against TGF- β 1. *PLoS One* 8: e82190. doi: [10.1371/journal.pone.0082190](#) PMID: [24349218](#)
4. Ito H, Hoshi M, Ohtaki H, Taguchi A, Ando K, Ishikawa T, et al. (2010) Ability of IDO to attenuate liver injury in alpha-galactosylceramide-induced hepatitis model. *J Immunol* 185: 4554–4560. doi: [10.4049/jimmunol.0904173](#) PMID: [20844202](#)
5. Hoshi M, Saito K, Hara A, Taguchi A, Ohtaki H, Tanaka R, et al. (2010) The absence of IDO upregulates type I IFN production, resulting in suppression of viral replication in the retrovirus-infected mouse. *J Immunol* 185: 3305–3312. doi: [10.4049/jimmunol.0901150](#) PMID: [20693424](#)
6. Ito H, Ando T, Ando K, Ishikawa T, Saito K, Moriwaki H, et al. (2014) Induction of HBsAg-specific cytotoxic T lymphocytes can be up-regulated by the inhibition of indoleamine 2, 3-dioxygenase activity. *Immunology*.
7. Iwamoto N, Ito H, Ando K, Ishikawa T, Hara A, Taguchi A, et al. (2009) Upregulation of indoleamine 2,3-dioxygenase in hepatocyte during acute hepatitis caused by hepatitis B virus-specific cytotoxic T lymphocytes in vivo. *Liver Int* 29: 277–283. doi: [10.1111/j.1478-3231.2008.01748.x](#) PMID: [18397228](#)
8. Ohtaki H, Ito H, Ando K, Ishikawa T, Hoshi M, Ando T, et al. (2014) Kynurenine production mediated by indoleamine 2,3-dioxygenase aggravates liver injury in HBV-specific CTL-induced fulminant hepatitis. *Biochim Biophys Acta* 1842: 1464–1471. doi: [10.1016/j.bbadis.2014.04.015](#) PMID: [24768802](#)
9. Moffett JR, Namboodiri MA (2003) Tryptophan and the immune response. *Immunol Cell Biol* 81: 247–265. PMID: [12848846](#)

10. Frumento G, Rotondo R, Tonetti M, Damonte G, Benatti U, Ferrara GB (2002) Tryptophan-derived catabolites are responsible for inhibition of T and natural killer cell proliferation induced by indoleamine 2,3-dioxygenase. *J Exp Med* 196: 459–468. PMID: [12186838](#)
11. Chung DJ, Rossi M, Romano E, Ghith J, Yuan J, Munn DH, et al. (2009) Indoleamine 2,3-dioxygenase-expressing mature human monocyte-derived dendritic cells expand potent autologous regulatory T cells. *Blood* 114: 555–563. doi: [10.1182/blood-2008-11-191197](#) PMID: [19465693](#)
12. Yan Y, Zhang GX, Gran B, Fallarino F, Yu S, Li H, et al. (2010) IDO upregulates regulatory T cells via tryptophan catabolite and suppresses encephalitogenic T cell responses in experimental autoimmune encephalomyelitis. *J Immunol* 185: 5953–5961. doi: [10.4049/jimmunol.1001628](#) PMID: [20944000](#)
13. Bahcecioglu IH, Yalniz M, Ataseven H, Bulbul N, Kececi M, Demirdag K, et al. (2004) TNF-alpha and leptin in experimental liver fibrosis models induced by carbon tetrachloride and by common bile duct ligation. *Cell Biochem Funct* 22: 359–363. PMID: [15386444](#)
14. Li D, Cai H, Hou M, Fu D, Ma Y, Luo Q, et al. (2012) Effects of indoleamine 2,3-dioxygenases in carbon tetrachloride-induced hepatitis model of rats. *Cell Biochem Funct* 30: 309–314. doi: [10.1002/cbf.2803](#) PMID: [22249930](#)
15. Lim HJ, Han J, Woo DH, Kim SE, Kim SK, Kang HG, et al. (2011) Biochemical and morphological effects of hypoxic environment on human embryonic stem cells in long-term culture and differentiating embryoid bodies. *Mol Cells* 31: 123–132. doi: [10.1007/s10059-011-0016-8](#) PMID: [21347709](#)
16. Chi V, Chandy KG (2007) Immunohistochemistry: paraffin sections using the Vectastain ABC kit from vector labs. *J Vis Exp*: 308.
17. Sakaida I, Matsumura Y, Akiyama S, Hayashi K, Ishige A, Okita K (1998) Herbal medicine Sho-saiko-to (TJ-9) prevents liver fibrosis and enzyme-altered lesions in rat liver cirrhosis induced by a choline-deficient L-amino acid-defined diet. *J Hepatol* 28: 298–306. PMID: [9514543](#)
18. Hoshi M, Ito H, Fujigaki H, Takemura M, Takahashi T, Tomita E, et al. (2009) Indoleamine 2,3-dioxygenase is highly expressed in human adult T-cell leukemia/lymphoma and chemotherapy changes tryptophan catabolism in serum and reduced activity. *Leuk Res* 33: 39–45. doi: [10.1016/j.leukres.2008.05.023](#) PMID: [18639341](#)
19. Ito H, Ando K, Ishikawa T, Saito K, Takemura M, Imawari M, et al. (2009) Role of TNF-alpha produced by nonantigen-specific cells in a fulminant hepatitis mouse model. *J Immunol* 182: 391–397. PMID: [19109170](#)
20. Zhang X, Yu WP, Gao L, Wei KB, Ju JL, Xu JZ (2004) Effects of lipopolysaccharides stimulated Kupffer cells on activation of rat hepatic stellate cells. *World J Gastroenterol* 10: 610–613. PMID: [14966928](#)
21. Kualess MA, Wenzel J, Schmid-Wendtner MH, Bieber T, von Bubnoff D (2011) Myeloid CD11c+ S100+ dendritic cells express indoleamine 2,3-dioxygenase at the inflammatory border to invasive lower lip squamous cell carcinoma. *Histol Histopathol* 26: 997–1006. PMID: [21692032](#)
22. Gressner AM, Lotfi S, Gressner G, Lahme B (1992) Identification and partial characterization of a hepatocyte-derived factor promoting proliferation of cultured fat-storing cells (parasinusoidal lipocytes). *Hepatology* 16: 1250–1266. PMID: [1427664](#)
23. Geerts A, Schellinck P, Bouwens L, Wisse E (1988) Cell population kinetics of Kupffer cells during the onset of fibrosis in rat liver by chronic carbon tetrachloride administration. *J Hepatol* 6: 50–56. PMID: [3346533](#)
24. Murata S, Maruyama T, Nowatari T, Takahashi K, Ohkohchi N (2014) Signal transduction of platelet-induced liver regeneration and decrease of liver fibrosis. *Int J Mol Sci* 15: 5412–5425. doi: [10.3390/ijms15045412](#) PMID: [24686514](#)
25. Sierra-Filardi E, Nieto C, Dominguez-Soto A, Barroso R, Sanchez-Mateos P, Puig-Kroger A, et al. (2014) CCL2 shapes macrophage polarization by GM-CSF and M-CSF: identification of CCL2/CCR2-dependent gene expression profile. *J Immunol* 192: 3858–3867. doi: [10.4049/jimmunol.1302821](#) PMID: [24639350](#)
26. Sato A, Nakashima H, Nakashima M, Ikarashi M, Nishiyama K, Kinoshita M, et al. (2014) Involvement of the TNF and FasL produced by CD11b Kupffer cells/macrophages in CCl4-induced acute hepatic injury. *PLoS One* 9: e92515. doi: [10.1371/journal.pone.0092515](#) PMID: [24667392](#)
27. Gressner AM (1996) Transdifferentiation of hepatic stellate cells (Ito cells) to myofibroblasts: a key event in hepatic fibrogenesis. *Kidney Int Suppl* 54: S39–45. PMID: [8731193](#)
28. Su GL (2002) Lipopolysaccharides in liver injury: molecular mechanisms of Kupffer cell activation. *Am J Physiol Gastrointest Liver Physiol* 283: G256–265. PMID: [12121871](#)
29. Chatamra K, Proctor E (1981) Phenobarbitone-induced enlargement of the liver in the rat: its relationship to carbon tetrachloride-induced cirrhosis. *Br J Exp Pathol* 62: 283–288. PMID: [7248170](#)

30. Tomasi A, Albano E, Banni S, Botti B, Corongiu F, Dessi MA, et al. (1987) Free-radical metabolism of carbon tetrachloride in rat liver mitochondria. A study of the mechanism of activation. *Biochem J* 246: 313–317. PMID: [2825631](#)
31. Dai Y, Cederbaum AI (1995) Inactivation and degradation of human cytochrome P4502E1 by CCl₄ in a transfected HepG2 cell line. *J Pharmacol Exp Ther* 275: 1614–1622. PMID: [8531136](#)
32. Murakami Y, Hoshi M, Hara A, Takemura M, Arioka Y, Yamamoto Y, et al. (2012) Inhibition of increased indoleamine 2,3-dioxygenase activity attenuates *Toxoplasma gondii* replication in the lung during acute infection. *Cytokine* 59: 245–251. doi: [10.1016/j.cyto.2012.04.022](#) PMID: [22609210](#)
33. Ogawa K, Hara T, Shimizu M, Ninomiya S, Nagano J, Sakai H, et al. (2012) Suppression of azoxy-methane-induced colonic preneoplastic lesions in rats by 1-methyltryptophan, an inhibitor of indoleamine 2,3-dioxygenase. *Cancer Sci* 103: 951–958. doi: [10.1111/j.1349-7006.2012.02237.x](#) PMID: [22320717](#)
34. Schmidt SK, Ebel S, Keil E, Woite C, Ernst JF, Benzin AE, et al. (2013) Regulation of IDO activity by oxygen supply: inhibitory effects on antimicrobial and immunoregulatory functions. *PLoS One* 8: e63301. doi: [10.1371/journal.pone.0063301](#) PMID: [23675474](#)
35. Feng Y, Siu KY, Ye X, Wang N, Yuen MF, Leung CH, et al. (2010) Hepatoprotective effects of berberine on carbon tetrachloride-induced acute hepatotoxicity in rats. *Chin Med* 5: 33. doi: [10.1186/1749-8546-5-33](#) PMID: [20849653](#)
36. Terness P, Bauer TM, Rose L, Dufter C, Watzlik A, Simon H, et al. (2002) Inhibition of allogeneic T cell proliferation by indoleamine 2,3-dioxygenase-expressing dendritic cells: mediation of suppression by tryptophan metabolites. *J Exp Med* 196: 447–457. PMID: [12186837](#)
37. Abu-Tair L, Axelrod JH, Doron S, Ovadya Y, Krizhanovsky V, Galun E, et al. (2013) Natural killer cell-dependent anti-fibrotic pathway in liver injury via Toll-like receptor-9. *PLoS One* 8: e82571. doi: [10.1371/journal.pone.0082571](#) PMID: [24340043](#)
38. Bataller R, Brenner DA (2005) Liver fibrosis. *J Clin Invest* 115: 209–218. PMID: [15690074](#)
39. Inagaki Y, Okazaki I (2007) Emerging insights into Transforming growth factor beta Smad signal in hepatic fibrogenesis. *Gut* 56: 284–292. PMID: [17303605](#)
40. Terao K, Ohkawa S, Miyagi Y, Morinaga S, Ohshige K, Yamamoto N, et al. (2013) Inflammation in background cirrhosis evokes malignant progression in HCC development from HCV-associated liver cirrhosis. *Scand J Gastroenterol* 48: 729–735. doi: [10.3109/00365521.2013.782064](#) PMID: [23556482](#)